Benzotriazole Adsorption and Inhibition of Cu(100) Corrosion in HCl: A Combined in Situ STM and in Situ FTIR Spectroscopy Study

M. R. Vogt,[†] R. J. Nichols,[‡] O. M. Magnussen,*[,†] and R. J. Behm[†]

Abteilung Oberflächenchemie und Katalyse, Universität Ulm, D-89069 Ulm, Germany, and Department of Chemistry, University of Liverpool, Donnan Laboratory, Liverpool L69 7 ZD

Received: February 19, 1998; In Final Form: May 12, 1998

The adsorption and the corrosion inhibiting effect of benzotriazole (BTAH) on Cu(100) electrodes in 0.1 M HCl were investigated using in situ STM, in situ FTIR spectroscopy, and electrochemical measurements. In the double-layer range up to potentials of −0.6 V vs SCE a Cu surface morphology with extended, atomically flat terraces, separated by almost randomly oriented steps, and a low Cu surface mobility are observed by STM. High-resolution STM images reveal a commensurate superstructure in this potential range, which is attributed to a chemisorbed adlayer of BTAH molecules. At potentials around −0.6 V this structure is replaced by a c(2 × 2) Cl^- adlayer, which has the same atomic and long-range structure as found in BTAH-free HCl solution. Upon further potential increase to potentials > −0.35 V STM experiments and polarization measurements indicate the onset of Cu dissolution, while the surface is still covered by the c(2 × 2) Cl^- adlayer. At slightly higher potentials (> −0.3 V) STM, IR, and electrochemical data point to the formation of a thick, inhibiting Cu(I)BTA film on the Cu surface. The pronounced differences of the BTAH adsorption behavior to that found in H_2SO_4 solution provide a microscopic explanation for the reduced inhibition efficiency of BTAH in the presence of chloride.

Introduction

For several decades benzotriazole ($C_6H_4N_3H$, BTAH) has been one of the most widely used corrosion inhibitors for copper and copper alloys as well as an important additive for Cu plating baths. As a result, the chemisorption of BTAH on clean copper, as well as on cuprous oxide surfaces, has been extensively investigated with ex situ and in situ techniques, under both electrochemical and ultrahigh-vacuum (UHV) conditions.[1−10] These studies revealed adsorption of a chemisorbed BTAH adlayer phase at low coverage (UHV) or at negative potentials, respectively.[2,3,7,9−11] At higher coverages or more positive potentials a multilayer phase formed by a polymerized Cu(I)-BTA complex was observed, which is thought to act as a corrosion protective barrier.[4,6,10−12]

Despite these numerous studies, considerable controversy exists on the process of film formation, on the inhibition mechanism, and on the adsorption geometry of BTAH on the clean or oxide-covered Cu substrate as well as on the chemical nature of the underlying electrode surface. Electrochemical studies on polycrystalline Cu electrodes have shown that the stability and thickness of the Cu(I)BTA film increases with pH and BTAH concentration and depends strongly on the nature of the anion.[11,13,14] In particular, it is well-known that the inhibition efficiency is strongly reduced in Cl^--containing solution. Here the inhibiting effect was on one hand attributed to the adsorption of BTAH on the electrode surface, followed by adsorption of a thin layer of the polymeric Cu(I)BTA phase on an oxide-free copper surface.[11,15] On the other hand, it was proposed that corrosion inhibition is due to a Cu_2O layer that grows on the electrode surface during the formation of Cu(I)-BTA and is stabilized by the latter phase.[12]

Information on the BTAH adsorption geometry was obtained in studies by surface-sensitive techniques, such as IR spectroscopy,[6] photoelectron spectroscopy,[16−19] and STM,[8,9] which were performed ex situ on emersed electrodes or on BTAH films grown in ultrahigh vacuum (UHV). On the basis of IR spectroscopic data on chemisorbed BTAH adlayers that were adsorbed on Cu covered by a cuprous oxide layer, it was proposed that the plane of the BTAH molecules is tilted with respect to the surface normal.[6] Finally, UHV-STM observations of BTAH gas-phase adsorption on clean and oxygen-covered Cu(110) revealed a c(4 × 2) structure on the bare Cu surface, suggesting flat adsorption of BTAH, and a disordered adlayer phase on surface areas covered by (2 × 1) O reconstruction.[8,9]

Recently, we reported first in situ STM observations of the surface structure and corrosion behavior of Cu(100) in BTAH-containing H_2SO_4 solution.[10] This was part of an ongoing study on the corrosion and corrosion inhibition of copper electrodes in sulfuric and hydrochloric acid solutions.[20−22] In that study two BTAH adlayer phases with different structures were found, namely a commensurate structure, which was attributed to a chemisorbed BTAH adlayer, and a chainlike molecular arrangement, which was associated with the polymeric Cu(I)BTA phase. In addition, time-resolved STM observations of the anodic dissolution of the BTAH-covered surfaces showed pronounced differences as compared to the dissolution in BTAH-free solution.

Here we present results of a combined in situ STM, in situ FTIR spectroscopy, and electrochemical study on the adsorption and corrosion inhibiting effect of BTAH on Cu(100) surfaces in 0.1 M HCl containing variable amounts of BTAH. On the basis of these results, it will be shown that with increasing potential three distinct adsorbate phases are observed, i.e., a

* To whom correspondence should be addressed.
[†] Universität Ulm.
[‡] University of Liverpool.

S1089-5647(98)01216-4 CCC: $15.00
Published on Web 06/29/1998

chemisorbed BTAH adlayer, a chloride adlayer, and, at sufficiently high BTAH concentrations, a thicker inhibiting Cu(I)BTA layer. The intermittent displacement of the BTAH adlayer by Cl^- as well as the process of Cu(I)BTA adlayer formation is distinctly different from the behavior found in H_2SO_4 solution,[10] which provides a microscopic explanation for the different inhibition efficiencies in the presence of these two anions.

Experimental Section

Sample and Electrolyte Preparation. The same Cu(100) single-crystal electrode was used for electrochemical, spectroscopic, and STM experiments. Before each measurement the Cu sample was electrochemically polished with 66% orthophosphoric acid for about 10 s at an anodic value between 1.8 and 2.4 V versus a platinum counter electrode. After etching, the crystal was thoroughly rinsed with ultrapure water (Millipore) and then immersed into the electrolyte at a potential between −0.7 and −0.8 V versus a SCE reference electrode. All potentials in the text are quoted against this electrode. Solutions were prepared from HCl (Merck, Suprapur), BTAH (Fluka, puriss.), and Millipore water. The detailed preparation procedures are described elsewhere.[21]

Electrochemical Measurements. Polarization curves and potential step experiments were recorded in a separate electrochemical cell using the dipping technique. To avoid current contributions from the edges of the crystal, these were additionally covered with Apiezon wax. Prior and during the measurements the electrolyte was purged with N_2. For the potential step experiments the electrode was kept for at least 15 min at −0.7 V before the potential was stepped to a value in the range −0.35 to 0 V.

FTIRS Experiments. Infrared spectroscopy measurements were carried out in Liverpool with a BioRad FTS40 spectrometer equipped with a liquid nitrogen cooled MCT detector using the SNIFTIRS (subtractively normalized interfacial Fourier transform infrared spectroscopy[23]) technique. A three-electrode cell with a CaF_2 IR window (spectral cutoff below 1000 cm^{-1}) was used for all spectroscopic experiments. After electropolishing, the Cu electrode, which was mounted on a special Teflon holder, was placed in the SNIFTIRS cell and aligned under potentiostatic control by pressing it against the IR window with a glass barrel. The thin-layer cell formed this way usually has a layer thickness of a few micrometers. For the measurements the potential was switched between two potentials E_1 and E_2, with IR reflectance spectra collected at each of the two potentials. Normalized spectra were obtained by taking the difference of the two spectra R_2 and R_1, divided by the reference spectra R_1 (always taken at $E_1 = -800$ mV). Thus, the normalized change in reflectance is given by $\Delta R/R = (R_2 - R_1)/R_1$. New species that are formed at potential E_2 and that are not present at E_1 give rise to new IR absorption bands. At these bands $\Delta R/R$ will be negative, since increased IR adsorption at E_2 is equivalent to decreased reflectivity at E_2, i.e., $(R_2 - R_1)/R_1 < 0$. In general, negative-going bands are related to species that are in excess at E_2, while positive-going ones correspond to species in excess at the reference potential E_1. The signal-to-noise ratio of the IR spectra was improved by collecting 1000 interferograms with a resolution of 4 cm^{-1} at each potential, from which the normalized spectrum $\Delta R/R$ was calculated.

STM. For the in situ STM experiments a home-built STM was used, which is described in detail elsewhere.[24] Tunneling tips were electrochemically etched from polycrystalline W wire in 2 M NaOH and subsequently coated with Apiezon wax or polypropylene, leaving only the very end of the tip exposed to the electrolyte. Tip and sample potentials were independently kept under potentiostatic control. In the experiments the Cu electrode was first immersed in pure 0.1 M HCl at a potential of −0.7 V, and the surface was checked by STM. Subsequently, the electrolyte was continuously changed under potential control to 0.1 M HCl + 75 mM BTAH. The STM images are presented as unfiltered top views with darker gray tones corresponding to lower surface areas.

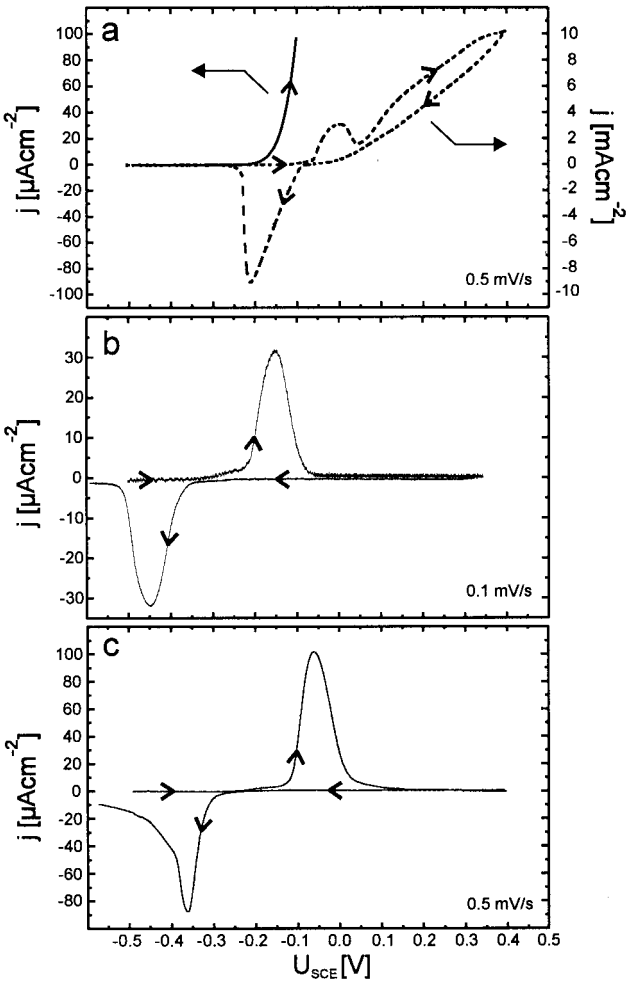

Figure 1. Polarization curves of Cu(100) in (a) 0.1 M HCl, (b) 0.1 HCl + 75 mM BTAH, and (c) 0.1 HCl + 10 mM BTAH. To show the high Cu dissolution current in the BTAH-free solution at potentials >0 V, the current density in (a) is also shown on an enlarged scale (dashed line).

Results

Electrochemical Characterization. Typical polarization curves of Cu(100) in 0.1 M HCl and 0.1 M HCl containing 75 or 10 mM BTAH, respectively, are shown in Figure 1. In the inhibitor-free solution an exponentially increasing Cu dissolution current is observed in the anodic scan at potentials positive of −0.2 V ("apparent Tafel region"), followed by a decrease in current above ≈0 V and a second increase above 0.05 V (Figure 1a). Similar behavior has been found previously in detailed electrochemical studies on the dissolution of polycrystalline Cu electrodes in chloride solutions.[11,25−30] The decrease in current between 0 and 0.05 V was attributed to the formation of a partly inhibiting CuCl film on the Cu surface. Upon reversal of the potential scan direction a broad cathodic peak centered at −0.2 V is observed, which corresponds to redeposition of Cu from the solution and/or the CuCl surface film.

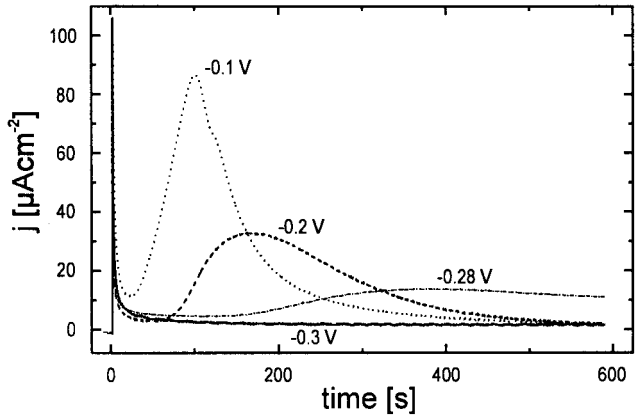

Figure 2. Current transients for Cu(100) in 0.1 M HCl + 75 mM BTAH after a potential step from −0.7 V to various potentials in the range of Cu(I)BTA film formation.

After adding 75 or 10 mM BTAH to the solution, the polarization behavior is totally different (Figure 1b,c). In both electrolytes a broad current peak is observed in the anodic potential scan. Positive of this peak the current is $<1\ \mu$A cm^{-2}, i.e., more than 3 orders of magnitude lower than in BTAH-free solution. This low current was observed up to values of 0.8 V. Reverse polarization results in a cathodic peak with almost identical charge, which is shifted by ≈0.29 V in negative direction relative to the anodic peak. In 75 mM BTAH the onset of the anodic current starts positive of −0.2 V, which is 0.15 V more negative than in BTAH-free solution, and peaks at −0.15 V. In 0.1 M HCl + 10 mM BTAH the behavior is similar, but the anodic and cathodic peaks are shifted by ≈0.1 V in positive direction with respect to the solution containing 75 mM BTAH. In both electrolytes the charge under the peaks is 17 ± 5 mC. A current peak corresponding to a slow film formation process is also observed in experiments where the potential was stepped to different values >-0.3 V (Figure 2). As can be expected, the rate of the film formation process increases with potential, but the total charge transfer is independent of the potential and approximately identical to that found in the polarization curves. Hence, the final thickness of the film is apparently independent of the polarization procedure. For 1 mM BTAH (not shown) the polarization curve was identical to that in pure HCl solution. This concentration dependence of the inhibition efficiency is in agreement with previous electrochemical data[13,31] and thermodynamic considerations.[32]

These results indicate (i) that in 0.1 M HCl solution containing ≥10 mM BTAH a corrosion protective film is formed on the copper crystal, which inhibits the dissolution of the underlying substrate, (ii) that the charge transfer associated with the formation of this film commences at distinctly more positive potentials than the Cu dissolution current in pure HCl solution, (iii) that this film can be completely reduced by negative polarization, and (iv) that the stable inhibiting film can be formed only if the BTAH concentration exceeds a certain critical value between 1 and 10 mM under the present conditions. Assuming a one-electron-transfer reaction for Cu dissolution in HCl solution[26] and a composition of Cu(I)BTA for the inhibiting film,[4,33] the charge under the peaks corresponds to the oxidation/reduction of ≈70 ± 20 Cu monolayers, equivalent to a film thickness of ≈200 ± 60 nm (calculated with a Cu(I)BTA density of 1.65 g cm^{-3} [4]).

Infrared Spectroscopy. To verify that the charge peaks obtained in BTAH-containing solution indeed correspond to the formation of a Cu(I)BTA layer, infrared spectroscopy experiments on Cu(100) in 0.1 M HCl + 75 mM BTAH were performed. SNIFTIRS spectra were recorded at stepwise increased potential E_2 in the potential range −0.7 to 0 V, while the potential of the reference spectra was held constant at −0.8 V. Selected normalized spectra are shown in Figure 3a. For potentials between −0.7 and −0.3 V no changes in the spectra are found. At potentials >-0.3 V several bands arise in the spectral region between 1350 and 1000 cm^{-1}, with positive-going bands at 1308, 1268, 1248, 1217, and 1014 cm^{-1} and negative ones at 1155 and 1119 cm^{-1}. Since these SNIFTIRS spectra are likely to contain bands arising from uncomplexed BTAH (which should be the main component at pH 2[11]) in the solution, it is first necessary to consider the assignment of the vibrational frequencies for BTAH. Previous IR spectroscopy studies on BTAH in both solution and solid phase[4,6,33] reported absorption peaks at frequencies identical to the positive bands observed in our experiment. Rubim et al.[33] assigned these bands predominantly to triazole stretching vibrations mixed with small contributions of C−H in-plane bending and ring stretching, In contrast, on the basis of detailed frequency calculations, Nilsson et al.[6] suggested that these bands correspond to almost pure C−H in-plane modes. Irrespective of the assignment, the occurrence of these bands implies that the concentration of BTAH in the thin layer decreases above −0.3 V. This decrease can result either from (i) adsorption of additional BTAH on

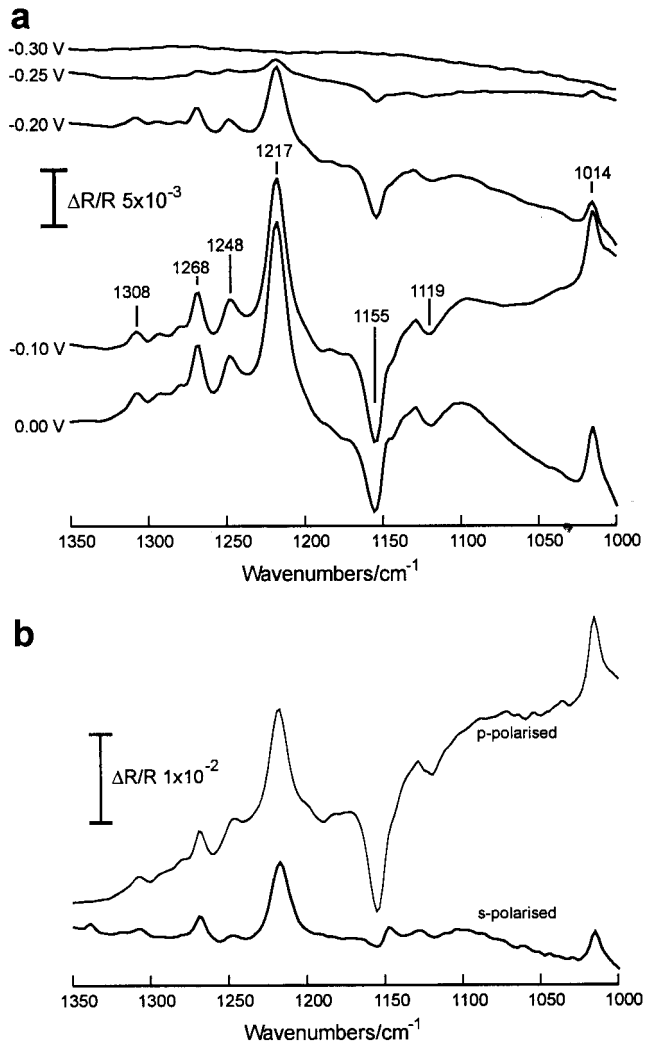

Figure 3. SNIFTIRS spectra of Cu(100) in 0.1 M HCl + 75 mM BTAH (−0.8 V reference potential) (a) at various potentials between −0.3 and 0.0 V. (b) s- and p-polarized SNIFTIRS spectra obtained at −0.1 V.

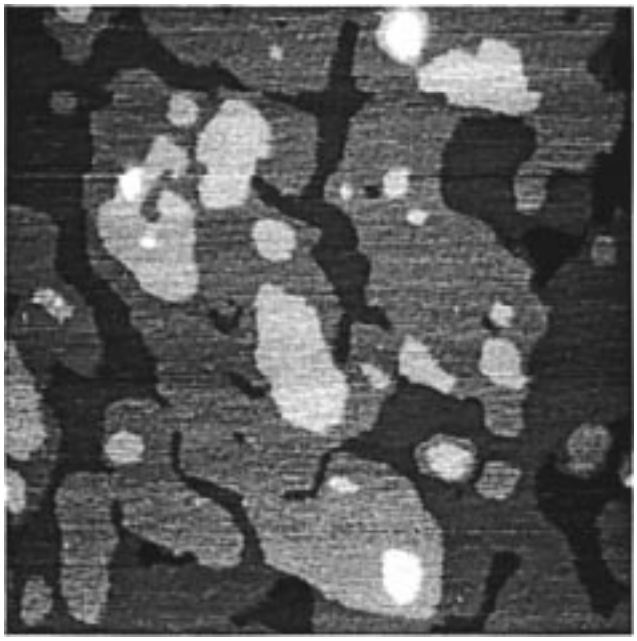

Figure 4. STM image of Cu(100) in 0.1 M HCl + 75 mM BTAH at −0.7 V, showing the typical long-range morphology for potentials <−0.6 V (1600 × 1600 Å, $I_t = 1$ nA).

the electrode surface at the higher potential or (ii) conversion of solution phase BTAH into a new chemical species.

The negative-going SNIFTIRS bands at 1155 and 1119 cm^{-1} are not found for BTAH but correspond closely to bands observed in spectra of a Cu(I)BTA complex embedded in a KBr matrix.[4,6] This suggests that the negative bands arise from Cu(I)BTA complexes that are formed after the anodic potential step to E_2. To distinguish between adsorbed and dissolved species, IR experiments with s- and p-polarized light were performed (Figure 3b). Bands corresponding to adsorbed species appear only in the spectra with p-polarized light, but not for s-polarized light, where the electric field vanishes at the surface. Dissolved species are detected with both polarizations.[34] The spectra show that the positive bands give spectral features in both s- and p-polarized spectra, while the negative bands appear only with p-polarized light. These results indicate that the Cu(I)BTA complex formed at positive potentials is adsorbed on the Cu(100) surface, while the BTAH must be present also in the solution.

STM. In the in situ STM measurements the Cu(100) electrode was initially imaged in pure 0.1 M HCl solution at the immersion potential of −0.7 V. Here the typical surface morphology with extended, atomically smooth terraces separated by randomly oriented, monatomic steps is observed, which was described previously.[20,21,35,36] After replacing the electrolyte by 0.1 M HCl + 75 mM BTAH, a similar nanometer scale morphology as in the pure HCl solution[20] is visible. In contrast to the latter, however, additional Cu monolayer islands and monatomically deep holes are found on the terraces (Figure 4). These additional islands and holes indicate BTAH-induced Cu dissolution and redeposition processes during the exchange procedure, which are currently not understood. The shape and position of these islands do not change significantly with time, indicating a low surface mobility. This differs distinctly from the observations in pure HCl solution, where STM measurements at similar potentials revealed a very high Cu surface mobility.[20]

These differences coincide with differences in the atomic scale surface structure in this potential regime. While in pure HCl solution the (1 × 1) lattice of the Cu substrate is observed,[20] an ordered superstructure is visible in the presence of BTAH (Figure 5a), which is attributed to a chemisorbed BTAH adlayer. The unit cell of this superstructure (indicated in Figure 5a) is nearly rectangular with unit cell vectors of 9.4 and 5.7 Å in length. In high-resolution STM images such as in Figure 5a, two maxima are discernible in each unit cell which are arranged along the long unit cell direction at a distance of ≈4.3 Å, leading to characteristic double-row-like features. The domains of this ordered structure are typically only 50−100 Å wide. Furthermore, structural defects in the domains and small disordered areas are frequently observed (Figure 5b). Four different rotational domains at angles of 90° and 52° to each other exist,[37] two of which are visible in Figure 5b. From these orientations as well as from the orientation with respect to the substrate axes, the structure can be identified as a

$$\begin{pmatrix} 2 & 1 \\ \bar{2} & 3 \end{pmatrix}$$

superstructure with unit cell vectors of $\sqrt{5}d_{Cu}$ and $\sqrt{13}d_{Cu}$ in length (with a Cu nearest-neighbor spacing $d_{Cu} = 2.56$ Å). The same structure was previously observed in BTAH-containing sulfuric acid solution,[10] however, without resolving the internal structure within the unit cell. Further information on the internal structure of this phase is obtained from an analysis of the translational domain boundaries. As can be seen in Figure 5a (arrows), the double rows split at the domain boundaries; i.e., the spacing of 4.3 Å between the maxima increases. This

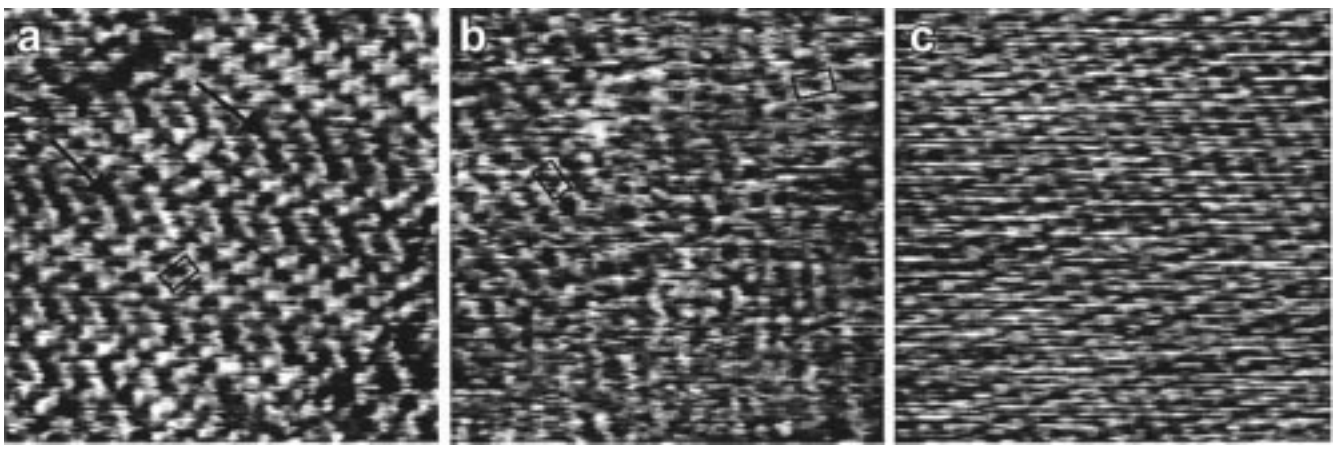

Figure 5. High-resolution STM images of Cu(100) in 0.1 M HCl + 75 mM BTAH, showing (a, b) the ordered, chemisorbed BTAH adlayer at −0.7 V (100 × 100 Å, $I_t = 0.4$ nA) and (c) the c(2 × 2)Cl adlayer at −0.45 V (75 × 75 Å, $I_t = 6$ nA).

observation indicates that the two maxima correspond to two individual adsorbates rather than to different parts of a single BTAH molecule. It also rules out an artifact of the STM imaging. Interestingly, these domain boundaries do not run parallel to the unit cell directions but at a characteristic angle of 45° to the direction of the double rows. The implications of the above observations for the adlayer structure will be discussed below.

At potentials > -0.6 V (Figure 5c) a different structure with a square lattice and a nearest-neighbor distance of 3.6 Å can be resolved, corresponding to a c(2 × 2) superstructure. This c(2 × 2) structure is well-known from STM studies of Cu(100) electrodes in BTAH-free HCl solution,[20,21,35,36] where it was formed in the same potential range[20,21] and where it is generally attributed to an ordered Cl^- adlayer. Simultaneously, a rearrangement of the surface morphology is observed, leading to atomically smooth Cu steps, which are almost perfectly orientated along the [010] and [001] directions (Figure 6a). The same step faceting process was also found in pure HCl solution and attributed to an adsorbate-induced restructuring of the Cu substrate.[20] Hence, the chemisorbed BTAH layer observed at negative potentials is completely displaced by the c(2 × 2) Cl^- adlayer at about −0.6 V. Returning to potential values < -0.6 V, the BTAH adlayer and the corresponding Cu substrate morphology with randomly oriented steps reappear; i.e., apart from a small hysteresis of 0.05 V, the potential-induced changes in the atomic and long-range surface structure are completely reversible. The same transition behavior albeit with different transition potentials was found at lower concentrations of BTAH or HCl.

Upon further increasing the potential ≥ -0.35 V dissolution of the copper electrode is observed. This is illustrated in Figure 6b, which was recorded in the same surface area as Figure 6a 2 min after the potential was increased from −0.4 to −0.3 V. Cu dissolution proceeds via a step-flow etching mechanism (examples marked by black arrows in the images). During the dissolution the step edges maintain their orientation along [010] and [001], and no significant roughening is observed. This dissolution mechanism is identical to that observed in pure HCl solution. The dominant ⟨001⟩ steps result from a stabilization by the c(2 × 2) Cl^- adlayer, whose close-packed direction is along ⟨001⟩. A detailed description of this mechanism is given elsewhere.[21] The onset of dissolution is shifted cathodically by about 0.1 V with respect to the inhibitor-free solution, in good agreement with the electrochemical measurements. As will be shown below, this can be explained by the presence of BTAH in the solution. At potentials positive of −0.2 V the STM images become foggy, and no stable imaging is possible. It was also not possible to obtain stable STM images after complete formation of the Cu(I)BTA film, i.e., at potentials positive of the current peaks in Figure 1b,c. Such behavior is very likely because of the poor electrical conductivity and the large thickness expected for this film. After complete dissolution of the thick Cu(I)BTA film at −0.7 V, stable images could be obtained again. Following these potential excursions the Cu surface exhibited a very rough large-scale morphology (Figure 7). In addition, many approximately circular hills with diameters of 50−130 Å are formed. These structural modifications require substantial Cu mass transfer during a Cu(I)BTA film formation/reduction cycle, which is in accordance with the interpretation of the electrochemical data. It is noteworthy that the smaller, hill-like structures resemble the morphology of Cu surfaces covered by an oxide film.

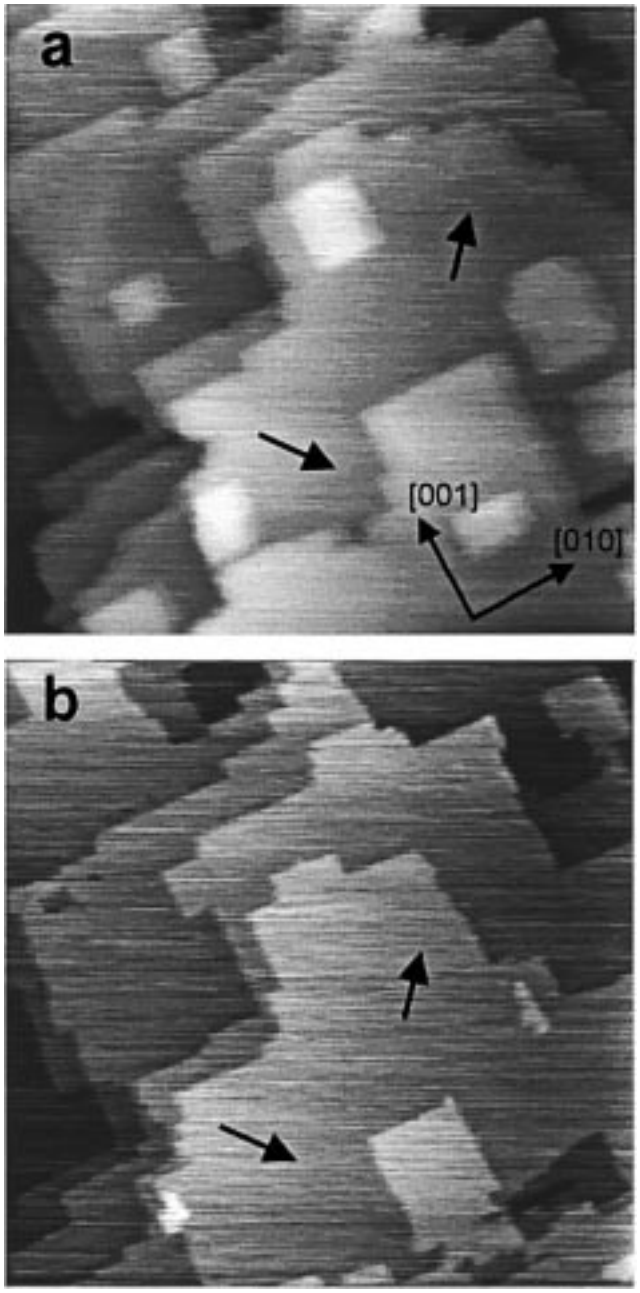

Figure 6. STM image of Cu(100) in 0.1 M HCl + 75 mM BTAH recorded in the same surface area (a) in the double-layer potential region at −0.40 V and (b) 2 min after the potential was increased from −0.4 to −0.3 V, showing the onset of Cu dissolution via a step flow mechanism (1600 × 1600 Å, $I_t = 1$ nA).

Discussion

The electrochemical, spectroscopic, and microscopic observations presented here give new insight into the adsorption of BTAH on Cu in HCl solution and its corrosion-inhibiting effect. In the following we will discuss in particular the structure of the chemisorbed BTAH adlayer at negative potentials, the influence of Cl^- on the interaction of BTAH with the Cu electrode surface, and the mechanism of Cu corrosion inhibition in HCl solution.

Our STM results clearly indicate the presence of a chemisorbed adlayer of BTAH on Cu(100) at potentials < -0.6 V, in agreement with previous spectroscopic data.[2,3] Although the absolute positions of the molecules with respect to the Cu lattice could not be determined by the STM measurements, this adlayer is apparently commensurate to the underlying metal substrate,

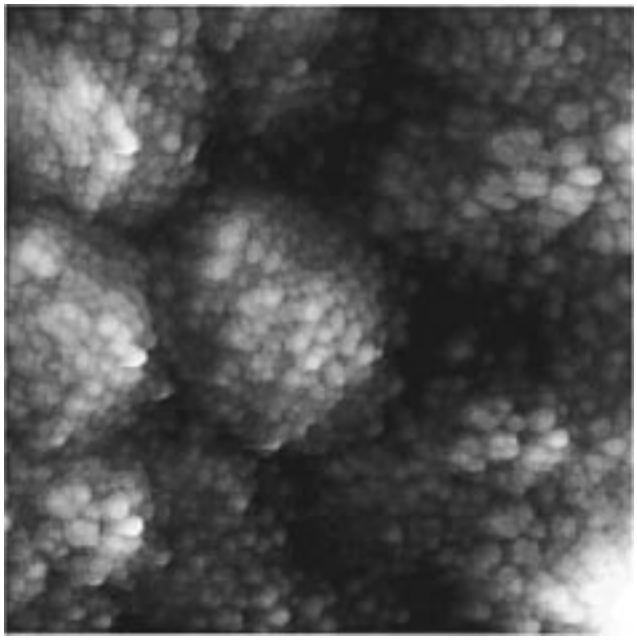

Figure 7. Morphology of Cu(100) in 0.1 M HCl + 75 mM BTAH after reduction (20 min at −0.7 V) of a Cu(I)BTA film, with the latter formed by keeping the potential for 15 min at +0.5 V (3000 × 3000 Å, I_t = 2.5 nA).

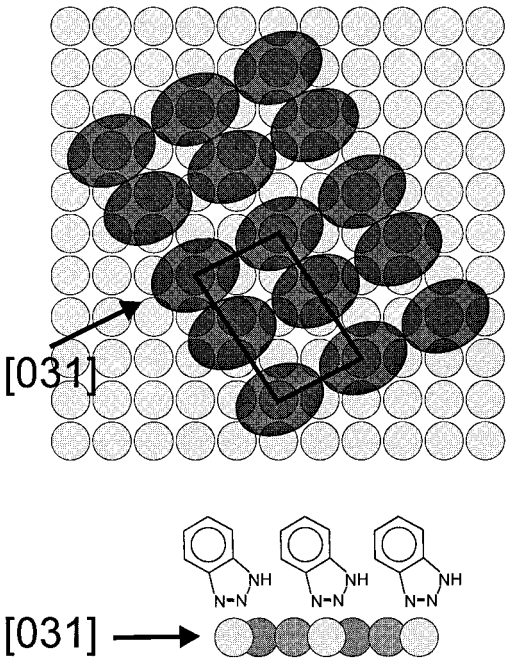

Figure 8. Model of the proposed structure of the BTAH adlayer on Cu(100). Due to the lack of data on the precise adsorption sites of the molecules, the positions of the molecules with respect to the Cu lattice are arbitrarily chosen.

indicating that the BTAH molecules occupy well-defined adsorption sites. The molecular spacing of 5.7 Å along one of the adlattice directions is also in good accordance with the lateral extension of BTAH along the molecular plane.[38] The spacing of 4.3 Å between the two molecules within the unit cell of the superstructure, however, cannot be matched by a Cu(100) lattice vector. Consequently, the apparent center of the two BTAH molecules must be located on different adsorption sites within the unit cell. On the other hand, the 4.3 Å spacing is almost identical to the minimum lattice spacing in crystalline BTAH and corresponds to an (almost) parallel stacking of the molecular planes.[38] In the adlayer a parallel stacking of the molecules can only be realized if the BTAH molecules are adsorbed perpendicular (or tilted at a small angle) to the surface. This adsorption geometry is also in accordance with previous spectroscopic data.[6,19] Since the 4.3 Å spacing is incommensurate with the Cu substrate lattice, a (low-order) commensurate adlattice can only be maintained by introducing a slightly larger spacing between every second row of molecules, resulting in pairing to double rows. Hence, the observed adlayer structure is a compromise between well-defined BTAH adsorption sites and maximum adlayer density.

The same superstructure was found previously on Cu(100) in BTAH-containing sulfuric acid solution, coexistent with a $(\sqrt{5} \times \sqrt{5})R26.6°$ structure.[10] In that study the two molecules within the superstructure unit cell were not individually resolved, and therefore a more open arrangement of BTAH in the adlayer was suggested. Since it is highly unlikely that the adlayers have an identical unit cell but a factor of 2 different density of BTAH molecules, we propose that the adsorption geometry described above, with parallel stacked BTAH molecules perpendicular (or tilted) to the Cu(100) surface, exists in both of the two different electrolytes. This suggests that the influence of the anions on the structure of the chemisorbed BTAH adlayer is small. A model for the proposed structure is shown in Figure 8. This model is distinctly different from that suggested for BTAH adsorbed on Cu(110) under UHV conditions,[7−9] the only other microscopic study on BTAH adlayer structures. In that study a more open c(4 × 2) structure was resolved by STM measurements, which led the authors to conclude that BTAH is adsorbed flat on the surface, followed by stand-up polymerization for BTAH coverages above one monolayer.[7]

At potentials > −0.6 V the atomic and long-range structure as well as the dynamic behavior of the Cu(100) surface are identical to that found in inhibitor-free HCl solution, indicating that the chemisorbed BTAH phase is completely displaced by adsorbing chloride ions. This transition occurs at the same potential where the transition from a disordered Cl^- adlayer to the c(2 × 2) phase is observed in pure 0.1 M HCl solution, which suggests that the replacement is correlated with the formation of the ordered Cl^- adlattice. (The difference in transition potential with respect to that given in refs 20 and 21 is caused by the different Cl^- concentrations.) Apparently, the same gain in energy that makes the c(2 × 2) Cl^- phase more favorable than a disordered Cl^- adlayer at potentials > −0.6 V also drives the displacement of the BTAH adlayer. In contrast, in sulfuric acid solution the Cu(100) surface is covered by a BTAH (or Cu(I)BTA) adlayer in the entire double-layer potential regime,[10] in agreement with the weaker adsorption of this anion.

This difference in the adsorption behavior of the inhibitor in the presence of the two different anions has a pronounced influence on the formation of the inhibiting Cu(I)BTA film, which can explain the well-known phenomenon of a reduced BTAH inhibition efficiency in chloride-containing solution. In HCl solution a direct conversion of the chemisorbed BTAH adlayer phase into the polymerized Cu(I)BTA phase, as reported previously for H_2SO_4 solution,[10] is not possible due to the intermittent formation of the c(2 × 2) Cl^- adlayer. On the c(2 × 2) Cl^- covered surface Cu dissolution can proceed in the same way as in BTAH-free HCl solution, and in fact the STM data show a similar step-flow dissolution mechanism in both cases. These findings suggest that in the initial stages of the dissolution process (i) BTAH or Cu(I)BTA is not present on the surface and (ii) the dissolution proceeds by the same reaction mechanism, namely the formation of $CuCl_2^-$ from $CuCl_{ads}$. The dissolution process is gradually inhibited by the

formation of the Cu(I)BTA film, which is evidenced by both potentiostatic and spectroscopic data.

These observations shed new light on the mechanism of Cu(I)BTA film formation and the related corrosion inhibition in chloride-containing solution, for which several conflicting models were proposed.[11,12,15,32] On the basis of electrochemical data and thermodynamical considerations, Tromans et al.[11] proposed that in 1 or 0.1 M NaCl solution containing 1 g/L BTAH the Cu(I)BTA film formation proceeds by the following sequence of reactions: First BTAH is chemisorbed on an oxide-free Cu surface. Subsequently, Cu(I)BTA in the diffusion layer, resulting from the reaction of $CuCl_2^-$ with BTAH, and the initial chemisorbed BTAH form a polymerized layer, which prevents the underlying substrate from dissolution. Based on photoelectrochemical measurements, a rather similar mechanism was proposed by Modestov et al.,[12] with the major difference that here the corrosion inhibition was attributed to a Cu(I)BTA-induced stabilization of a Cu_2O layer, formed underneath the Cu(I)BTA film. Our in situ results in combination with the previous data[11,15,32] lead to the following picture for the formation mechanism of the inhibiting film: Film formation starts with the production of $CuCl_2^-$ ions via the same reaction as in BTAH-free solution. These $CuCl_2^-$ ions react with BTAH in the solution to Cu(I)BTA, which subsequently precipitates on the Cu surface and thus forms the inhibiting layer. The cathodic potential shift of the Cu dissolution with respect to BTAH-free solution is related to the corresponding (BTAH-induced) depletion in the $CuCl_2^-$ concentration. Most important, the Cu(100) surface is clearly covered by a c(2 × 2) Cl^- adlayer in the initial stages of this process, although it is still unclear whether this adlayer is replaced by the Cu(I)BTA film or incorporated into it.

Summary

In summary, we have presented a study by the complementary techniques of in situ STM, in situ IR spectroscopy, and electrochemical measurements on BTAH adsorption and on the induced corrosion inhibition of Cu(100) electrodes in 0.1 M HCl solution containing 75−10 mM BTAH. At potentials <0.6 V a chemisorbed BTAH adlayer with commensurate structure is found, which was also observed in previous experiments in sulfuric acid solution. Due to the higher microscopic resolution achieved in the present study, a refined structural model of this adlayer phase is developed, where the molecular plane is perpendicular or slightly tilted with respect to the surface normal. At potentials >-0.6 V the adsorbed BTAH is reversibly replaced by a c(2 × 2) chloride adlayer. This new adlayer phase is observed on the Cu(100) surface up to the onset of Cu dissolution at potentials >-0.35 V. The $CuCl_2^-$ ions formed during the latter process react with BTAH in the solution to Cu(I)BTA, which subsequently precipitates and thus covers the Cu surface with an inhibiting film. This mechanism significantly differs from that found in BTAH-containing H_2SO_4 solution, where the chemisorbed BTAH adlayer is directly transformed into the Cu(I)BTA phase, providing a microscopic explanation for the reduced inhibition efficiency of BTAH in chloride-containing solution.

Acknowledgment. We gratefully acknowledge financial support and a fellowship for O.M.M. by the Deutsche Forschungsgemeinschaft. M.R.V. received a research fellowship by the DAAD.

References and Notes

(1) Cotton, J. B.; Scholes, I. R. *Br. Corros. J.* **1967**, *2*, 1.
(2) Youda, R.; Nishihara, H.; Aramaki, K. *Electrochim. Acta* **1990**, *35*, 1011.
(3) Youda, R.; Nishihara, H.; Aramaki, K. *Corros. Sci.* **1988**, *28*, 87.
(4) Poling, G. W. *Corros. Sci.* **1970**, *10*, 359.
(5) Hope, G. A.; Schweinsberg, D. P.; Fredericks, P. M. *Spectrochim. Acta* **1994**, *50A*, 2019.
(6) Nilsson, J.-O.; Törnkvist, C.; Liedberg, B. *Appl. Surf. Sci.* **1989**, *37*, 306.
(7) Park, J.; Noh, H.; Kuk, Y.; Cho, K.; Sakurai, T. *J. Korean Phys. Soc.* **1996**, *29*, 745.
(8) Cho, K.; Kishimoto, J.; Hashizume, T.; Pickering, H. W.; Sakurai, T. *Appl. Surf. Sci.* **1995**, *87/88*, 380.
(9) Cho, K.; Kishimoto, J.; Hashizume, T.; Sakurai, T. *Jpn. J. Appl. Phys.* **1994**, *33*, L125.
(10) Vogt, M. R.; Polewska, W.; Magnussen, O. M.; Behm, R. J. *J. Electrochem. Soc.* **1997**, *144*, L113.
(11) Tromans, D.; Sun, R. *J. Electrochem. Soc.* **1991**, *138*, 3235.
(12) Modestov, A. D.; Zhou, G. D.; Wu, Y. P.; Notoya, T.; Schweinsberg, D. P. *Corros. Sci.* **1994**, *36*, 1931.
(13) Walker, R. *Corrosion* **1973**, *29*, 290.
(14) El-Taib Heakal, F.; Haruyama, S. *Corros. Sci.* **1980**, *20*, 887.
(15) Tromans, D.; Silva, J. C. *Corrosion* **1997**, *53*, 16.
(16) Chadwick, D.; Hashemi, T. *Corros. Sci.* **1978**, *18*, 39.
(17) Roberts, R. F. *J. Electron Spectrosc. Relat. Phenom.* **1974**, *4*, 273.
(18) Hashemi, T.; Hogarth, C. A. *Electrochim. Acta* **1988**, *33*, 1123.
(19) Fang, B. S.; Olson, C. G.; Lynch, D. W. *Surf. Sci.* **1986**, *176*, 476.
(20) Vogt, M. R.; Möller, F. A.; Schilz, C. M.; Magnussen, O. M.; Behm, R. J. *Surf. Sci.* **1996**, *367*, L33.
(21) Vogt, M. R.; Lachenwitzer, A.; Magnussen, O. M.; Behm, R. J. *Surf. Sci.* **1998**, *399*, 49.
(22) Scherer, J.; Vogt, M. R.; Magnussen, O. M.; Behm, R. J. *Langmuir* **1997**, *13*, 7045.
(23) Pons, S.; Davidson, T.; Bewick, A. *J. Electroanal. Chem.* **1984**, *160*, 63.
(24) Wiechers, J.; Twomey, T.; Kolb, D. M.; Behm, R. J. *J. Electroanal. Chem.* **1988**, *248*, 451.
(25) Bacarella, A. L.; Griess, J. C. *J. Electrochem. Soc.* **1973**, *120*, 459.
(26) Lee, H. P.; Nobe, K. *J. Electrochem. Soc.* **1986**, *133*, 2035.
(27) Modestov, A. D.; Zhou, G.; Ge, H.; Loo, B. H. *J. Electroanal. Chem.* **1995**, *380*, 63.
(28) Braun, M.; Nobe, K. *J. Electrochem. Soc.* **1979**, *126*, 1666.
(29) D'Elia, E.; Barcia, O. E.; Mattos, O. R.; Pebere, N.; Tribollet, B. *J. Electrochem. Soc.* **1996**, *143*, 961.
(30) Lee, H. P.; Nobe, K.; Pearlstein, A. J. *J. Electrochem. Soc.* **1985**, *132*, 1031.
(31) Fox, P. G.; Lewis, G.; Boden, P. J. *Corros. Sci.* **1979**, *19*, 457.
(32) Tromans, D. *J. Electrochem. Soc.* **1998**, *145*, L42.
(33) Rubim, J.; Gutz, I. G. R.; Sala, O.; Orville-Thomas, W. J. *J. Mol. Struct.* **1983**, *100*, 571.
(34) Iwasita, T.; Nart, F. C. In *Advances in Electrochemical Science and Engineering*; Gerischer, H., Tobias, C. W., Eds.; VCH: Weinheim, 1990; p 123.
(35) Suggs, D. W.; Bard, A. J. *J. Phys. Chem.* **1995**, *99*, 8349.
(36) Moffat, T. P. *Mat. Res. Soc. Symp. Proc.* **1997**, *451*, 75.
(37) Note that the angle in ref 10 between the different rotational domains were mistakingly given as 90° and 20°.
(38) Escande, P. A.; Galigné, J. L.; Lapasset, J. *Acta Crystallogr.* **1974**, *B30*, 1490.